

Toxic Misfolded Transthyretin Oligomers with Different Molecular Conformations Formed through Distinct Oligomerization Pathways

Anvesh K. R. Dasari, Sujung Yi, Matthew F. Coats, Sungsool Wi, and Kwang Hun Lim*



Cite This: *Biochemistry* 2022, 61, 2358–2365



Read Online

ACCESS |



Metrics & More

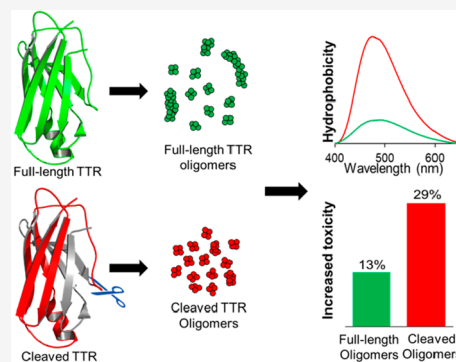


Article Recommendations



Supporting Information

ABSTRACT: Protein aggregation is initiated by structural changes from native polypeptides to cytotoxic oligomers, which form cross- β structured amyloid. Identification and characterization of oligomeric intermediates are critically important for understanding not only the molecular mechanism of aggregation but also the cytotoxic nature of amyloid oligomers. Preparation of misfolded oligomers for structural characterization is, however, challenging because of their transient, heterogeneous nature. Here, we report two distinct misfolded transthyretin (TTR) oligomers formed through different oligomerization pathways. A pathogenic TTR variant with a strong aggregation propensity (L55P) was used to prepare misfolded oligomers at physiological pH. Our mechanistic studies showed that the full-length TTR initially forms small oligomers, which self-assemble into short protofibrils at later stages. Enzymatic cleavage of the CD loop was also used to induce the formation of N-terminally truncated oligomers, which was detected in ex vivo cardiac TTR aggregates extracted from the tissues of patients. Structural characterization of the oligomers using solid-state nuclear magnetic resonance and circular dichroism revealed that the two TTR misfolded oligomers have distinct molecular conformations. In addition, the proteolytically cleaved TTR oligomers exhibit a higher surface hydrophobicity, suggesting the presence of distinct oligomerization pathways for TTR oligomer formation. Cytotoxicity assays also revealed that the cytotoxicity of cleaved oligomers is stronger than that of the full-length TTR oligomers, indicating that hydrophobicity might be an important property of toxic oligomers. These comparative biophysical analyses suggest that the toxic cleaved TTR oligomers formed through a different misfolding pathway may adopt distinct structural features that produce higher surface hydrophobicity, leading to the stronger cytotoxic activities.



Protein misfolding and aggregation are implicated in diverse degenerative disorders such as Alzheimer's disease and amyloidosis.^{1–4} Misfolding and aggregation are initiated by structural changes from native polypeptides to oligomeric intermediate states, which eventually form cross- β structured amyloid.^{1–4} Although the identity of toxic species formed during the aggregation process remains the subject of active debate, mounting evidence suggests that small oligomeric species rather than mature fibrils are responsible for cellular dysfunction.^{5–14} Identification and structural analyses of oligomeric intermediates are, therefore, critical for understanding the cytotoxic properties of misfolded oligomers. Structural characterization of misfolded oligomers would also be essential to developing biomarkers and molecular imaging probes that can detect misfolded oligomers formed at an initial stage of protein misfolding disorders.^{15–17}

Transthyretin (TTR) is a 55 kDa homotetramer that binds and transports thyroxine in the plasma and cerebrospinal fluid.^{18,19} TTR misfolding and aggregation are linked to amyloidosis (ATTR), which impacts numerous organs, including the peripheral nerves and heart. Amyloid deposition of wild-type (WT) TTR is linked to amyloid cardiomyopathy (ATTR-CM), affecting as much as 25% of the population over

age 80.^{20–23} More than 120 single-point mutations were observed in patients with earlier onset of amyloid cardiomyopathy [hereditary ATTR-CM (hATTR-CM)].²⁴ Aggregation of the TTR variants was also observed in the peripheral and autonomic nerves, causing amyloid polyneuropathy (ATTR-PN) in ~50000 patients worldwide.^{25,26} ATTR amyloidosis was originally believed to be a rare disease, but it is now well recognized that amyloidosis is underdiagnosed and significantly more prevalent than previously thought.^{27,28}

Previous biochemical studies of ATTR amyloidosis revealed that native TTR tetramers are dissociated into monomers, which undergo a structural change to a partly folded intermediate that self-associates into oligomers and subsequently amyloid.^{29–31} On the basis of the mechanistic studies, therapeutic agents that can stabilize native tetramers were

Received: July 1, 2022

Revised: October 3, 2022

Published: October 11, 2022



developed to prevent the dissociation of the native TTR.³² The TTR stabilizers, including tafamidis, were shown to delay the development of disease and improve the quality of life of ATTR patients at early stages of the disease.^{33,34} Thus, early diagnosis of ATTR amyloidosis is essential to the effective treatment of ATTR patients. Currently, most diagnostic tools for ATTR amyloidosis are focused on detecting amyloid fibrils deposited on tissues.³⁵ Development of biomarkers that can detect misfolded oligomeric species formed at an initial stage of aggregation would be critically important in the treatment of ATTR amyloidosis.

Isolation and structural analyses of misfolded TTR oligomers are essential for developing biomarkers and molecular imaging probes. In this study, two distinct misfolded TTR oligomers were prepared for the biophysical studies by using a full-length pathogenic TTR variant with a strong aggregation propensity (L55P)^{36,37} that might allow us to prepare a large amount of oligomers for the structural studies. In addition to the full-length TTR, N-terminally truncated TTR (residues 49–127) produced by an enzymatic cleavage was used to produce misfolded oligomers because *ex vivo* TTR amyloids extracted from the tissues of patients contain the N-terminally truncated TTR.^{38,39} The N-terminally truncated TTR oligomers were also detected in the plasma of hATTR patients,¹⁶ supporting that aggregation of the cleaved TTR is also physiologically relevant.

The full-length TTR oligomers (L55P) were obtained by incubating the purified protein at physiological pH and temperature (37 °C). The proteolytic cleavage of the TTR also accelerated misfolding and aggregation, as was previously demonstrated,^{40–42} resulting in the formation of small oligomers. The biophysical properties of the TTR oligomers, such as cytotoxicity and hydrophobicity, were investigated to gain insights into the correlation between cytotoxicity and hydrophobicity. Interestingly, the truncated TTR oligomers (residues 49–127) with higher hydrophobicity exhibited stronger cytotoxic activity than the full-length TTR oligomers. Our comparative structural analyses using solid-state nuclear magnetic resonance (NMR) and circular dichroism (CD) also revealed that the truncated TTR oligomers adopt molecular structures different from those of the full-length TTR oligomers, suggesting that the more toxic oligomers may have distinct structural features that exhibit higher surface hydrophobicity.

MATERIALS AND METHODS

Preparation of Recombinant TTR. Protein expression was carried out using a bacterial expression system with the L55P TTR plasmid (pMMHa, a gift from Dr. Kelly at Scripps), as previously described.⁴³ *Escherichia coli* cells (BL21) were cultured in M9 medium containing ¹⁵N-enriched NH₄Cl and [¹³C]glucose under constant 250 rpm agitation at 37 °C. The cells were grown until the optical density at 600 nm reached 0.7–0.8, and TTR overexpression was induced with 1 mM isopropyl β-D-1-thiogalactopyranoside. After incubation for an additional 12–14 h at 25 °C, the cells were harvested via centrifugation. The bacterial pellet was dissolved using Tris lysis buffer [10 mM Tris and 150 mM NaCl (pH 8.0)], and the resuspended solution was sonicated to disrupt the bacterial pellet. The soluble fraction was collected via centrifugation, and high-molecular weight impurities were removed by ammonium sulfate precipitation (50 wt %/vol). The supernatant saved via centrifugation was dialyzed overnight against

Tris buffer [25 mM Tris, 1 mM PMSF, and 1 mM EDTA (pH 8.0)] at 4 °C. The protein was further purified by using an anion exchange column [HiTrap Q HP; 20 mM Tris and 1 mM EDTA (pH 8.0)] and gel filtration chromatography with a size exclusion column [HiLoad 16/60 Superdex 75 pg; 10 mM sodium phosphate buffer (pH 7.4)].

Preparation of TTR Oligomers. The purified full-length proteins [5–15 mg/mL in 10 mM PBS buffer (pH 7.4)] were incubated under constant agitation at 250 rpm and 37 °C to induce oligomerization of L55P TTR. To obtain the cleaved TTR (residues 49–127) oligomers, full-length L55P TTR (15 μM) was incubated with trypsin using a ratio of 200:1 (w/w) for 5 days.

Transmission Electron Microscopy (TEM). Three microliters of the incubated TTR solution was placed on a glow-discharged Formvar/carbon-coated copper 400 mesh grid and incubated for 30 s. A filter paper was used to remove excess solution, and the grids were washed with deionized water. The grids were stained with 1% uranyl acetate and incubated for 30 s. Excess stain was removed using filter paper, and the samples were then dried in air. CM12 Philips TEM at an electron energy of 80 kV was used to obtain TEM images. To examine reproducibility of oligomer formation, a whole TEM grid was examined for the samples prepared with three independent experiments.

Cell Viability Assay. SH-SY5Y neuroblastoma cells were cultured in a 1:1 mixture of 1% Pen-Strep and DMEM/F12 medium with 10% FBS at 37 °C in a humidified atmosphere with 5% CO₂. The growth medium was replaced every 5 days. SH-SY5Y cells with a density of 10 000 cells per well were plated in a 96-well plate. The mammalian cells were allowed to settle on the plate for 24 h, and the cell medium was renewed with fresh medium containing the TTR oligomers at different concentrations. After incubation for 48 h, the cells in a fresh medium were treated with MTT, which were then incubated for an additional 4 h. Sodium dodecyl sulfate (SDS) was added to the cells, and the optical density was recorded at 570 nm using a microplate reader (SpectraMax) after 4 h. All of the experiments were carried out in duplicate.

Fluorescence Experiments. A thioflavin T fluorescence assay was used to monitor TTR aggregation kinetics with and without trypsin. The TTR variant (0.3 and 0.7 mg/mL) was incubated with 10 μM thioflavin T in a clear bottom microplate. The microplate was shaken at 250 rpm and 37 °C. The ThT fluorescence was recorded for different incubation periods using a microplate reader (SpectraMax) with excitation and emission wavelengths of 482 and 440 nm, respectively.

For ANS binding experiments, a 20 μM ANS solution was prepared in 10 mM PBS buffer (pH 7.4). TTR oligomers were mixed with the ANS working solution to a final protein concentration of 10 μM. The emission spectra were recorded between 400 and 650 nm using a 1 mm slit width with a 350 nm excitation wavelength.

Circular Dichroism (CD) Spectroscopy. All CD spectra were recorded using a protein concentration of 0.2 mg/mL (monomeric TTR concentration). Far-ultraviolet CD spectra from 190 to 260 nm were recorded using a Jasco J-815 CD spectrometer with a 1 mm quartz cuvette. An average of 20 scans was acquired for each sample.

Solid-State NMR. Two-dimensional (2D) solid-state NMR spectra were recorded using a Bruker 800 MHz NMR spectroscope and a 3.2 mm magic-angle-spinning (MAS) probe. The NMR experiments were performed at an MAS

frequency of 12 kHz, and a dipolar-assisted rotational resonance (DARR)⁴⁴ was used for the mixing scheme in the 2D experiments. Then, 1024 × 256 complex data points were collected for all of the samples, and 128 FIDs were accumulated for each t1 data point with an acquisition delay of 2 s. TopSpin 4.0 and Sparky 3.1⁴⁵ were used to process and analyze the NMR data.

RESULTS

Preparation of Small TTR Oligomers. Previous biophysical studies of TTR misfolding and aggregation suggested that dissociation of the tetramer into amyloidogenic monomers is a rate-determining step in the TTR aggregation, and the dissociation is accelerated under more acidic conditions with an optimum pH of ~4.^{43,46} Previous structural studies have, therefore, been mainly focused on misfolded TTR aggregates formed under mildly acidic conditions. In this study, a TTR variant with strong aggregation propensity (L55P)³⁶ was employed to prepare misfolded oligomers at neutral pH because pathogenic mutations were shown to promote the dissociation of the native tetramers, accelerating misfolding and aggregation.⁴⁷ The pathogenic TTR variant (5 mg/mL) with strong aggregation propensity was incubated at 37 °C to induce the formation of misfolded oligomers at physiological pH. Size exclusion chromatography (SEC) was employed to probe oligomers present in the protein solution incubated at 37 °C and pH 7.4 (red in Figure 1a). After a short incubation

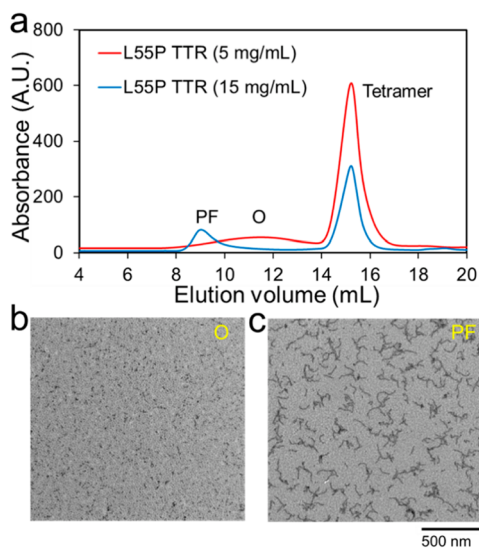


Figure 1. (a) Size exclusion chromatography (SEC) analysis of L55P TTR. Purified L55P TTR [in 10 mM PBS buffer (pH 7.4)] was incubated at different concentrations, 5 and 15 mg/mL, to afford oligomers (O) and protofibrils (PF), respectively. TEM images of the purified (b) oligomers and (c) protofibrils.

period (1 day), small oligomers eluting at ~12 mL were observed for the TTR variant. Larger oligomeric species appear to form after a longer incubation of 14 days (Figure S1).

The morphology of the oligomeric species was investigated by TEM (Figure 1b and Figure S2a), which revealed small spherical oligomers with a diameter of ~5 nm. After the longer incubation, larger oligomeric species (protofibrils) were also observed in addition to small oligomers, suggesting that the small oligomeric species self-assemble into the protofibrils (Figure S1), as was previously observed for wild-type TTR

oligomers formed under mildly acidic conditions (pH 4.4).⁴⁸ To confirm the formation of protofibrils, the TTR variant was incubated at a higher concentration of 15 mg/mL at pH 7.4 (blue in Figure 1a). The larger oligomeric species eluting at ~10 mL via SEC were examined via TEM, revealing the formation of protofibrils (Figure 1c and Figure S2b). Long fibrillar aggregates were, however, not observed even after prolonged incubation times. These results suggest that the TTR variant forms small oligomeric species that aggregate into curly protofibrils instead of long filamentous fibrillar aggregates.

TTR Oligomers Formed by Enzymatic Cleavage. TTR misfolding and aggregation were shown to be accelerated by the enzymatic cleavage of the CD loop (residues 48 and 49).^{40–42} Our previous studies also revealed that the proteolytic cleavage effectively induces TTR misfolding and aggregation at physiological pH.⁴² Thus, the pathogenic TTR variant (L55P) was treated with trypsin to prepare misfolded N-terminally truncated TTR. Aggregation rates of L55P TTR incubated with trypsin are greatly increased (Figure 2a),

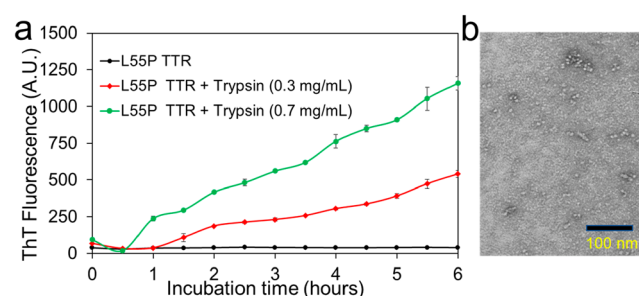


Figure 2. (a) Aggregation kinetics of L55P TTR (pH 7.4) with and without trypsin. The enzymatic cleavage for the K48–T49 peptide bond was confirmed by MS and SDS gel (Figure S3). (b) TEM image of the cleaved TTR oligomers. ThT fluorescence was measured at 482 nm with an excitation wavelength of 440 nm to examine the aggregation kinetics. The errors were calculated from two independent experiments.

consistent with the previous observations. Interestingly, TEM analyses of the incubated TTR samples revealed the presence of small oligomers (Figure 2b and Figure S4). After long incubations, larger oligomeric species and fibrillar aggregates were not detected in contrast to the full-length oligomers, suggesting that the small oligomers were formed through an oligomerization pathway different from that of the full-length TTR variant (Figure 1).

Characterization of the Small TTR Oligomers.

Cytotoxic activities of the full-length and N-terminally cleaved oligomers were examined by using a 3-(4,5-dimethylthiazol-2-yl)-2,5-diphenyltetrazolium bromide (MTT) assay (Figure 3a). The viability assays reveal that the oligomers formed by the enzymatic cleavage (cleaved, green) exhibited stronger cytotoxic activity compared to that of the full-length TTR oligomers (red). It was previously shown that surface hydrophobicity is correlated well with the toxicity of the misfolded oligomers.⁴⁹ The ANS (8-anilino-1-naphthalenesulfonic acid) fluorescence assay was, therefore, used to compare the hydrophobicity of the oligomers (Figure 3b). The higher fluorescence intensity of the cleaved oligomers (green) clearly indicates that the cleaved TTR oligomers have larger hydrophobic surfaces, consistent with their stronger cytotoxic properties.

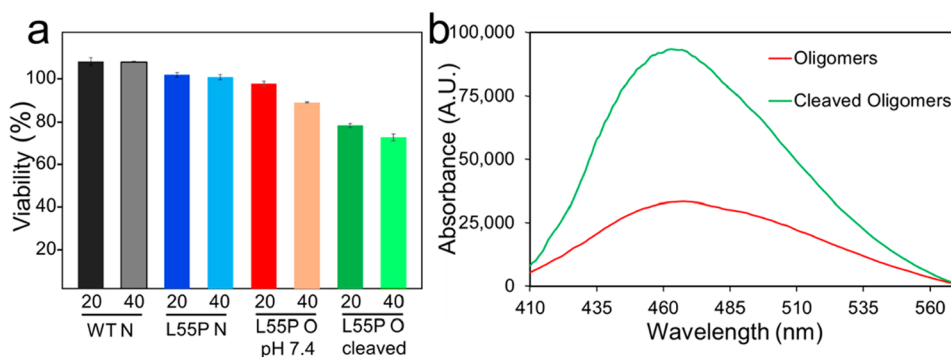


Figure 3. (a) MTT cell viability assay for the native (N) and oligomeric (O) states tested at different TTR concentrations (monomer concentrations of 20 and 40 μM). (b) ANS fluorescence spectra of purified L55P oligomers (red, oligomers; green, cleaved oligomers). TTR oligomers (5 μM) were mixed with 20 μM ANS [in 10 mM PBS buffer (pH 7.4)], and the fluorescence emission spectra were recorded with an excitation wavelength of 350 nm.

Structural Features of the Small TTR Oligomers. Our TEM analyses revealed that small oligomeric species appear to self-assemble into larger oligomers. CD spectroscopy was used for comparative structural analyses of the small oligomers and protofibrils formed by the full-length TTR at different incubation periods (Figure 4). The native TTR is rich in β -

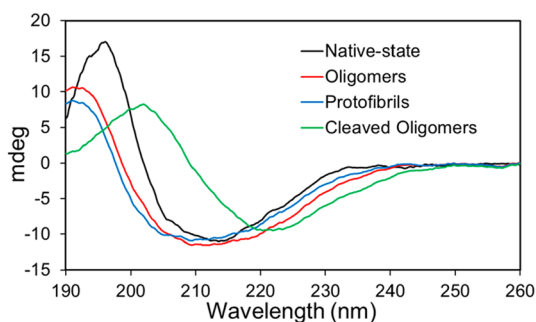


Figure 4. CD spectra of the L55P TTR oligomers (0.14 mg/mL) in 10 mM phosphate buffer (pH 7.4). Spectra were recorded at 20 $^{\circ}\text{C}$ using a Jasco-815 CD spectrometer with a 1 mm quartz cuvette. The full-length oligomers and protofibrils were obtained after incubation for 1 day and 3 weeks, respectively.

structures, as evidenced by a maximum at ~ 195 nm and a minimum at ~ 215 nm (black). In the full-length TTR small oligomers (red), the magnitudes of the CD signals in the low-wavelength regions are significantly decreased compared with those of the native state, suggesting that the TTR oligomers become more unstructured than the native state. However, the strong signal at ~ 215 nm in the full-length TTR oligomer spectrum similar to that of the native state indicates that the full-length oligomers contain extensive β -structures. It is also notable that the CD spectrum for the protofibrils (blue) is almost identical to that of the small oligomers (red), suggesting that no major conformational changes are accompanied by the self-assembly of the oligomers into the protofibrils. On the contrary, oligomeric species formed by the enzymatic cleavage at pH 7.4 (green) exhibit a quite distinct CD spectrum with a maximum at ~ 206 nm and a minimum of ~ 222 nm, suggesting that the cleaved oligomers adopt molecular structures distinct from those of the full-length oligomers.

Solid-state NMR is well-suited for comparative structural analyses of the full-length L55P oligomers and native tetramer (Figure 5a) because the ^{13}C NMR chemical shifts of the

aliphatic carbons are highly sensitive to the local environments.^{50,51} The 2D NMR spectra obtained with a dipolar-assisted-rotational-resonance (DARR)⁴⁴ mixing scheme show that the NMR cross-peaks from the full-length L55P TTR oligomers (red) are similar to those of the native TTR tetramer (black). However, many NMR cross-peaks in the native state disappeared in the oligomer spectra, suggesting that TTR may undergo local conformational changes. Indeed, the resonance assignment of the native state⁵² revealed that most cross-peaks absent in the full-length oligomer spectrum correspond to those of EF helix/loop regions (pink in panels a and c of Figure 5), suggesting that the helical region undergoes conformational changes during oligomerization. Single-point mutations that destabilize the helical regions were also shown to promote TTR misfolding and aggregation.⁵³ These results indicate that local structural changes of the EF helix/loop regions are critical to misfolding and aggregation of TTR.

In addition to the EF helix/loop, many cross-peaks from the residues in the tetrameric interfaces (AB and GH loops) of the native state (blue in panels a and c of Figure 5) are absent in the full-length TTR oligomer spectrum, suggesting reorganization of the monomers in the misfolded oligomers. The new NMR resonances observed for the full-length oligomers (asterisk in Figure 5a) may originate from those regions that undergo local conformational changes and/or new interfacial regions in the misfolded oligomers. These NMR results suggest that the monomers in the full-length TTR oligomers have overall native-like β -structures with substantial non-native local structures and non-native interfacial regions. The native-like monomers may adopt non-native oligomers with distinct interfaces from those of the native tetramers.

Molecular conformations of the proteolytically cleaved L55P oligomers (green) were also compared with those of the native TTR (black, Figure 5b). NMR cross-peaks from several amino acid residues such as Thr, Val, and Ala are still overlapped. However, more than half of the NMR cross-peaks in the native state, including the EF helix/loop and AB and GH loops, disappeared in the cleaved oligomer spectrum. The NMR resonances from the CD and DE loop (brown, Figure 5b,d) are also absent in the cleaved oligomer spectrum, indicating that the enzymatic cleavage of the CD loop induces more drastic conformational changes and the cleaved oligomers adopt non-native molecular conformations. The NMR results are consistent with the substantial differences observed in the

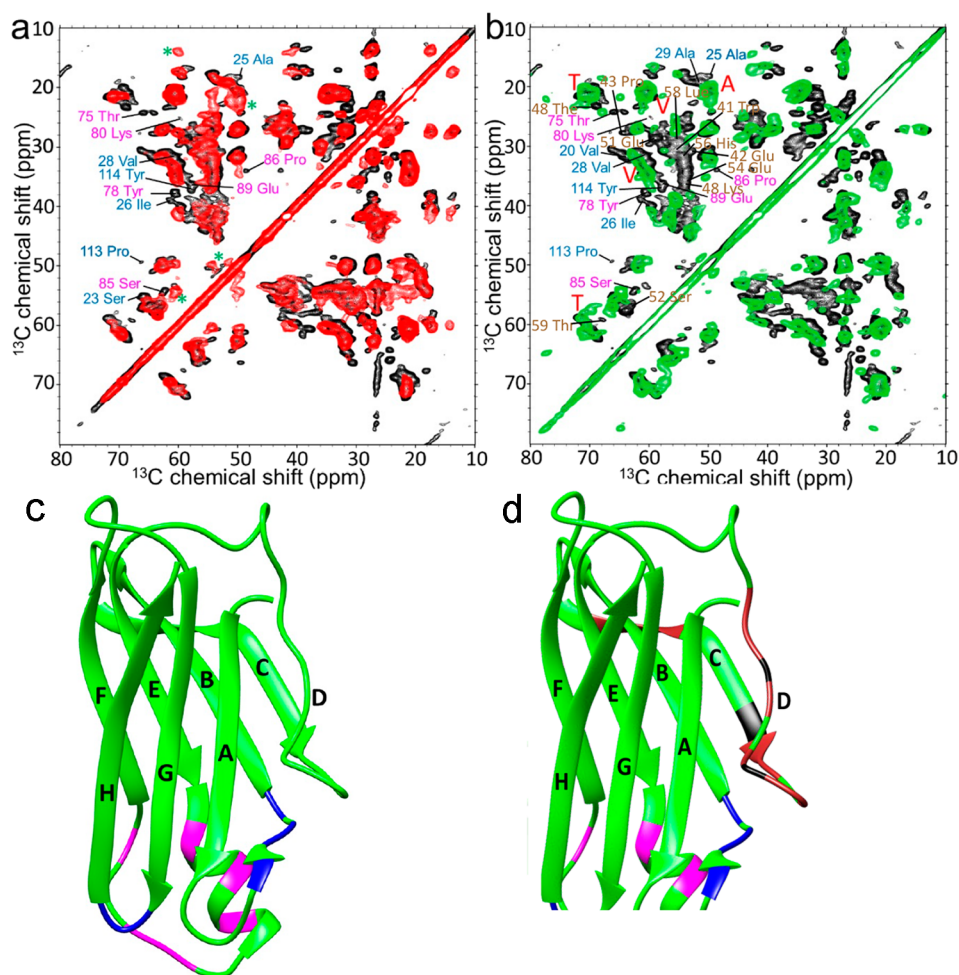


Figure 5. (a) Aliphatic regions of the ^{13}C -detected 2D solid-state NMR DARR spectra for the L55P native (black) and full-length oligomers (red). (b) Overlaid 2D spectra for the native L55P TTR (black) and L55P TTR oligomers formed by enzymatic cleavage (green). (c) Crystal structure of the L55P TTR monomer (Protein Data Bank entry 3DJZ) with colored residues in the tetrameric interface (AB and GH loops, blue) and EF helix/loop (magenta) that disappeared in the full-length TTR oligomer NMR spectrum. (d) Crystal structure with colored residues in the loop regions [AB and GH, EF helix/loop, and CD and DE loops (brown)] that disappeared in the cleaved TTR oligomer NMR spectrum. A DARR mixing time of 20 ms was used for the 2D solid-state NMR spectra. The NMR samples were collected and packed into 3.2 mm MAS rotors by ultracentrifugation. The oligomer samples inside the rotor have remained stable, reproducing the identical NMR spectra. The NMR assignments of the cross-peaks are made on the basis of our previous backbone assignment of the native TTR.⁵²

CD spectra for the native state (black) and cleaved TTR oligomers (green, Figure 4).

DISCUSSION

Structural characterization of misfolded protein oligomers is quite difficult because of the transient and heterogeneous nature.^{5,8,54–56} The preparation of diverse misfolded oligomers with differential cytotoxic activities is essential for exploring the cytotoxic nature of the misfolded oligomers. It was previously shown that TTR amyloids consisting of the N-terminally truncated as well as full-length TTR were found in the tissues of patients. The C-terminal fragment produced by the enzymatic cleavage of the K48–T49 peptide bond was shown to be the main TTR fragment,^{39,57–59} indicating that enzymatic cleavage may result in aggregation of the N-terminally cleaved TTR fragment. Indeed, previous studies revealed that enzymatic digestions of the K48–T49 peptide bond in the TTR variants (E51_S52dup and S52P) lead to the formation of TTR amyloids containing the N-terminally truncated fragment (residues 49–127).^{40,41} A very recent

study also showed that ex vivo TTR aggregates (V122I) containing the N-terminally truncated fragment are thermodynamically and morphologically similar to those of the in vitro 49–127 TTR aggregates prepared by enzymatic cleavage.⁵⁸ In addition, the N-terminally truncated TTR oligomers were detected in the plasma of hATTR patients,¹⁶ supporting that aggregation of the cleaved TTR might be physiologically relevant. In this study, misfolded TTR oligomers formed by the full-length and proteolytically cleaved TTR were, therefore, prepared for comparative biophysical analyses.

The full-length TTR variant (L55P) initially formed small oligomers with a diameter of ~ 5 nm at an early stage of aggregation, which then self-assemble into protofibrils after longer incubations. The enzymatic cleavage of the CD loop also induced the formation of small oligomeric species, but the small oligomers did not aggregate into larger aggregates under the experimental conditions used in this study. Our structural analyses of the TTR oligomers revealed that the small oligomers formed by the enzymatic cleavage adopt molecular

structures distinct from those of the full-length oligomers, suggesting the presence of distinct oligomerization pathways for the TTR variant. Our biophysical analyses also revealed that the N-terminally cleaved oligomers exhibit higher surface hydrophobicity, which might lead to stronger cytotoxicity. These results suggested that the more toxic cleaved oligomers adopt distinct molecular conformations with higher surface hydrophobicity.

Our experimental data are generally consistent with previous results. First, it was previously shown that cytotoxic activities of the six amyloid oligomers formed from three polypeptides, β -amyloid ($A\beta$) peptides, α -synuclein, and the N-terminal domain of HypF from *E. coli* (HypF-N), correlated well with their surface hydrophobicity.⁴⁹ These results suggest that the extent of the exposed hydrophobic surface is a critical parameter for toxic misfolded oligomers. The hydrophobic regions of the oligomers may play important roles in cellular dysfunctions through aberrant interactions with lipid membranes and/or various cellular proteins involved in signaling pathways.

Second, helical amyloidogenic intermediates have been previously observed during misfolding and aggregation of intrinsically disordered proteins, including α -synuclein,^{60,61} suggesting that helical secondary structures may play an important role in cytotoxic activities of misfolded oligomers. However, recent comparative structural analyses of toxic and nontoxic misfolded oligomers revealed that the formation of specific secondary structures like β -sheet is not a prerequisite for cytotoxic properties of misfolded oligomers.⁶² Our structural analyses using CD spectroscopy showed that the full-length TTR oligomers are substantially β -structured with some disordered regions, which is consistent with our previous solid-state NMR structural studies using selective labeling schemes.^{63,64} However, the truncated TTR oligomers with higher cytotoxicity have nonhelical secondary structures quite distinct from those of the full-length TTR oligomers and other helical amyloidogenic intermediates. These results are in line with previous observations that suggest differences in secondary structures are not enough to account for cytotoxic activities of misfolded oligomers. More detailed structural characterization of the toxic oligomers is required to unravel tertiary and quaternary structural features that exhibit enhanced surface hydrophobicity.

Atomic structures of the ex vivo TTR fibrils extracted from an ATTR patient's heart and vitreous body of the eye were recently determined by cryo-electron microscopy (cryo-EM).^{65,66} The cryo-EM structures revealed that TTR undergoes conformational changes from the natively folded β -barrel structures to disc-like 2D flat layers. The structural changes involve various loop regions, including AB, CD, DE, and GH loops and the EF helix/loop. In particular, unfolding of the CD loop in the native state was proposed to be a critical step for TTR fibril formation.⁶⁶ The structural rearrangement is consistent with our NMR results for the cleaved TTR oligomers, which revealed structural changes in the loop regions (pink, blue, and brown in Figure 5d). In addition, the two ex vivo TTR fibrils consist of the full-length and N-terminally truncated TTR, including the fragment of residues 49–127. Our TTR oligomers formed by the enzymatic cleavage also contain both the full-length and N-terminally truncated fragments (Figure S3b). These results suggest that the enzymatic cleavage of the CD loop may accelerate the tetramer dissociation and the N-terminally truncated mono-

mers can coaggregate with the full-length monomers. More detailed structural investigation of the cleaved oligomers would be required for thorough comparative structural analyses.

CONCLUSION

Distinct misfolded oligomeric species formed by the N-terminally truncated and full-length L55P TTR were prepared for biophysical and structural characterization. Biophysical analyses of the TTR oligomers revealed that the proteolytically cleaved oligomers have a higher surface hydrophobicity, exhibiting stronger cytotoxic properties. Comparative structural analyses revealed that the full-length TTR oligomers have extensive native-like β -structures with non-native interfacial regions, while the proteolytically cleaved oligomers adopt distinct non-native molecular structures from those of the full-length oligomers. These results suggest that detailed structural characterization of quaternary structures of misfolded oligomers is required to explore enhanced surface hydrophobicity, which is critical for understanding their cytotoxic properties. Finally, the full-length oligomers were able to self-assemble into protofibrils, while the proteolytically cleaved oligomers remained as small oligomers under our experimental conditions, suggesting that the two oligomers were formed through different oligomerization pathways.

ASSOCIATED CONTENT

Supporting Information

The Supporting Information is available free of charge at <https://pubs.acs.org/doi/10.1021/acs.biochem.2c00390>.

A SEC profile for TTR oligomerization, TEM images of the oligomers and protofibrils, and the mass spectrum and SDS gel for the cleaved TTR (PDF)

Accession Codes

Transthyretin, UniProtKB entry P02766.

AUTHOR INFORMATION

Corresponding Author

Kwang Hun Lim – Department of Chemistry, East Carolina University, Greenville, North Carolina 27858, United States; orcid.org/0000-0002-0971-200X; Email: limk@ecu.edu

Authors

Anvesh K. R. Dasari – Department of Chemistry, East Carolina University, Greenville, North Carolina 27858, United States; orcid.org/0000-0001-7248-1876

Sujung Yi – Department of Chemistry, East Carolina University, Greenville, North Carolina 27858, United States

Matthew F. Coats – Department of Chemistry, East Carolina University, Greenville, North Carolina 27858, United States

Sungsool Wi – Interdisciplinary Magnetic Resonance (CIMAR), National High Magnetic Field Laboratory (NHMFL), Tallahassee, Florida 32310, United States

Complete contact information is available at:

<https://pubs.acs.org/doi/10.1021/acs.biochem.2c00390>

Author Contributions

A.K.R.D., S.Y., and M.F.C. prepared the protein samples and conducted CD and toxicity experiments. S.W. carried out solid-state NMR experiments. K.H.L. designed and analyzed the experimental data. A.K.R.D. and K.H.L. wrote the manuscript.

Funding

This work was funded by National Institutes of Health Grant R01-NS097490 to K.H.L., and the National High Magnetic Field Laboratory is supported by the State of Florida and the National Science Foundation through NSF/DMR-1644779.

Notes

The authors declare no competing financial interest.

ABBREVIATIONS

NMR, nuclear magnetic resonance; TTR, transthyretin; TEM, transmission electron microscopy; CD, circular dichroism; SEC, size exclusion chromatography; DARR, dipolar-assisted rotational resonance; MTT, 3-(4,5-dimethylthiazol-2-yl)-2,5-diphenyltetrazolium bromide; ANS, 8-anilino-1-naphthalene-1-sulfonate; ThT, thioflavin T; MAS, magic-angle spinning.

REFERENCES

- (1) Ke, P. C.; Zhou, R.; Serpell, L. C.; Riek, R.; Knowles, T. P. J.; Lashuel, H. A.; Gazit, E.; Hamley, I. W.; Davis, T. P.; Fändrich, M.; Otzen, D. E.; Chapman, M. R.; Dobson, C. M.; Eisenberg, D. S.; Mezzenga, R. Half a century of amyloids: Past, present and future. *Chem. Soc. Rev.* **2020**, *49*, 5473–5509.
- (2) Dobson, C. M. Protein folding and misfolding. *Nature* **2003**, *426*, 884–890.
- (3) Chiti, F.; Dobson, C. M. Protein misfolding, functional amyloid, and human disease. *Annu. Rev. Biochem.* **2006**, *75*, 333–366.
- (4) Jahn, T. R.; Radford, S. E. Folding versus aggregation: Polypeptide conformations on competing pathways. *Arch. Biochem. Biophys.* **2008**, *469*, 100–117.
- (5) Glabe, C. G. Structural classification of toxic amyloid oligomers. *J. Biol. Chem.* **2008**, *283*, 29639–29643.
- (6) Laganowsky, A.; Liu, C.; Sawaya, M. R.; Whitelegge, J. P.; Park, J.; Zhao, M.; Pensalfini, A.; Soriaga, A. B.; Landau, M.; Teng, P. K.; Cascio, D.; Glabe, C.; Eisenberg, D. Atomic view of a toxic amyloid small oligomer. *Science* **2012**, *335*, 1228–1231.
- (7) Stefani, M. Structural features and cytotoxicity of amyloid oligomers: Implications in Alzheimer's disease and other diseases with amyloid deposits. *Prog. Neurobiol.* **2012**, *99*, 226–245.
- (8) Fändrich, M. Oligomeric intermediates in amyloid formation: Structure determination and mechanisms of toxicity. *J. Mol. Biol.* **2012**, *421*, 427–440.
- (9) Chen, S. W.; Drakulic, S.; Deas, E.; Ouberaï, M.; Aprile, F. A.; Arranz, R.; Ness, S.; Roodveldt, C.; Williams, T.; De-Genst, E. J.; Klenerman, D.; Wood, N. W.; Knowles, T. P.; Alfonso, C.; Rivas, G.; Abramov, A. Y.; Valpuesta, J. M.; Dobson, C. M.; Cremades, N. Structural characterization of toxic oligomers that are kinetically trapped during alpha-synuclein fibril formation. *Proc. Natl. Acad. Sci. U. S. A.* **2015**, *112*, 1994.
- (10) Reixach, N.; Deechongkit, S.; Jiang, X.; Kelly, J. W.; Buxbaum, J. N. Tissue damage in the amyloidoses: Transthyretin monomers and nonnative oligomers are the major cytotoxic species in tissue culture. *Proc. Natl. Acad. Sci. U. S. A.* **2004**, *101*, 2817–2822.
- (11) Fusco, G.; Chen, S. W.; Williamson, P. T. F.; Cascella, R.; Parni, M.; Jarvis, J. A.; Cecchi, C.; Vendruscolo, M.; Chiti, F.; Cremades, N.; Ying, L.; Dobson, C. M.; De Simone, A. Structural basis of membrane disruption and cellular toxicity by alpha-synuclein oligomers. *Science* **2017**, *358*, 1440–1443.
- (12) Ke, P. C.; Zhou, R.; Serpell, L. C.; Riek, R.; Knowles, T. P. J.; Lashuel, H. A.; Gazit, E.; Hamley, I. W.; Davis, T. P.; Fändrich, M.; Otzen, D. E.; Chapman, M. R.; Dobson, C. M.; Eisenberg, D. S.; Mezzenga, R. Half a century of amyloids: Past, present and future. *Chem. Soc. Rev.* **2020**, *49*, 5473–5509.
- (13) Cascella, R.; Chen, S. W.; Bigi, A.; Camino, J. D.; Xu, C. K.; Dobson, C. M.; Chiti, F.; Cremades, N.; Cecchi, C. The release of toxic oligomers from alpha-synuclein fibrils induces dysfunction in neuronal cells. *Nat. Commun.* **2021**, *12*, 1814.
- (14) Hou, X.; Parkington, H. C.; Coleman, H. A.; Mechler, A.; Martin, L. L.; Aguilar, M. I.; Small, D. H. Transthyretin oligomers induce calcium influx via voltage-gated calcium channels. *J. Neurochem.* **2007**, *100*, 446–457.
- (15) El-Agnaf, O. M.; Salem, S. A.; Paleologou, K. E.; Curran, M. D.; Gibson, M. J.; Court, J. A.; Schlossmacher, M. G.; Allsop, D. Detection of oligomeric forms of alpha-synuclein protein in human plasma as a potential biomarker for Parkinson's disease. *FASEB J.* **2006**, *20*, 419–425.
- (16) Schonhoft, J. D.; Monteiro, C.; Plate, L.; Eisele, Y. S.; Kelly, J. M.; Boland, D.; Parker, C. G.; Cravatt, B. F.; Teruya, S.; Helmke, S.; Maurer, M.; Berk, J.; Sekijima, Y.; Novais, M.; Coelho, T.; Powers, E. T.; Kelly, J. W. Peptide probes detect misfolded transthyretin oligomers in plasma of hereditary amyloidosis patients. *Sci. Transl. Med.* **2017**, *9*, eam7621.
- (17) Jiang, X.; Labaudinière, R.; Buxbaum, J. N.; Monteiro, C.; Novais, M.; Coelho, T.; Kelly, J. W. A circulating, disease-specific, mechanism-linked biomarker for ATTR polyneuropathy diagnosis and response to therapy prediction. *Proc. Natl. Acad. Sci. U. S. A.* **2021**, *118*, e2016072118.
- (18) Buxbaum, J. N.; Reixach, N. Transthyretin: The servant of many masters. *Cell. Mol. Life Sci.* **2009**, *66*, 3095–3101.
- (19) Herbert, J.; Wilcox, J. N.; Pham, K. T.; Freneau, R. T., Jr; Zeviani, M.; Dwork, A.; Soprano, D. R.; Makover, A.; Goodman, D. S.; Zimmerman, E. A.; et al. Transthyretin: A choroid plexus-specific transport protein in human brain. the 1986 S. Weir Mitchell award. *Neurology* **1986**, *36*, 900–911.
- (20) Westermark, P.; Sletten, K.; Johansson, B.; Cornwell, G. G., 3rd. Fibril in senile systemic amyloidosis is derived from normal transthyretin. *Proc. Natl. Acad. Sci. U.S.A.* **1990**, *87*, 2843–2845.
- (21) Coelho, T.; Maurer, M. S.; Suhr, O. B. THAOS - the transthyretin amyloidosis outcomes survey: Initial report on clinical manifestations in patients with hereditary and wild-type transthyretin amyloidosis. *Curr. Med. Res. Opin.* **2013**, *29*, 63–76.
- (22) Westermark, P.; Bergstrom, J.; Solomon, A.; Murphy, C.; Sletten, K. Transthyretin-derived senile systemic amyloidosis: Clinicopathologic and structural considerations. *Amyloid* **2003**, *10* (Suppl. 1), 48–54.
- (23) Herrick, M. K.; DeBruyne, K.; Horoupian, D. S.; Skare, J.; Vanefsky, M. A.; Ong, T. Massive leptomeningeal amyloidosis associated with a Val30Met transthyretin gene. *Neurology* **1996**, *47*, 988–992.
- (24) Ruberg, F. L.; Grogan, M.; Hanna, M.; Kelly, J. W.; Maurer, M. S. Transthyretin amyloid cardiomyopathy: JACC state-of-the-art review. *J. Am. Coll. Cardiol.* **2019**, *73*, 2872–2891.
- (25) Connors, L. H.; Richardson, A. M.; Theberge, R.; Costello, C. E. Tabulation of transthyretin (TTR) variants as of 1/1/2000. *Amyloid* **2000**, *7*, 54–69.
- (26) João, M.; Saraiva, M. Transthyretin mutations in health and disease. *Hum. Mutat.* **1995**, *5*, 191–196.
- (27) Manolis, A. S.; Manolis, A. A.; Manolis, T. A.; Melita, H. Cardiac amyloidosis: An underdiagnosed/underappreciated disease. *Eur. J. Int. Med.* **2019**, *67*, 1–13.
- (28) Rubin, J.; Maurer, M. S. Cardiac amyloidosis: Overlooked, underappreciated, and treatable. *Annu. Rev. Med.* **2020**, *71*, 203–219.
- (29) Lai, Z. H.; Colon, W.; Kelly, J. W. The acid-mediated denaturation pathway of transthyretin yields a conformational intermediate that can self-assemble into amyloid. *Biochemistry* **1996**, *35*, 6470–6482.
- (30) Lashuel, H. A.; Lai, Z. H.; Kelly, J. W. Characterization of the transthyretin acid denaturation pathways by analytical ultracentrifugation: Implications for wild-type, V30M, and L55P amyloid fibril formation. *Biochemistry* **1998**, *37*, 17851–17864.
- (31) Quintas, A.; Vaz, D. C.; Cardoso, I.; Saraiva, M. J.; Brito, R. M. Tetramer dissociation and monomer partial unfolding precedes protofibril formation in amyloidogenic transthyretin variants. *J. Biol. Chem.* **2001**, *276*, 27207–27213.
- (32) Rosenblum, H.; Castano, A.; Alvarez, J.; Goldsmith, J.; Helmke, S.; Maurer, M. S. TTR (transthyretin) stabilizers are associated with

- improved survival in patients with TTR cardiac amyloidosis. *Circ. Heart Failure* **2018**, *11*, e004769.
- (33) Müller, M. L.; Butler, J.; Heidecker, B. Emerging therapies in transthyretin amyloidosis - a new wave of hope after years of stagnancy? *Eur. J. Heart Fail.* **2020**, *22*, 39–53.
- (34) Johnson, S. M.; Wiseman, R. L.; Sekijima, Y.; Green, N. S.; Adamski-Werner, S. L.; Kelly, J. W. Native state kinetic stabilization as a strategy to ameliorate protein misfolding diseases: A focus on the transthyretin amyloidosis. *Acc. Chem. Res.* **2005**, *38*, 911–921.
- (35) Benson, M. D.; Dasgupta, N. R.; Rao, R. Diagnosis and screening of patients with hereditary transthyretin amyloidosis (hATTR): Current strategies and guidelines. *Ther. Clin. Risk Manag.* **2020**, *16*, 749–758.
- (36) Lashuel, H. A.; Wurth, C.; Woo, L.; Kelly, J. W. The most pathogenic transthyretin variant, L55P, forms amyloid fibrils under acidic conditions and protofilaments under physiological conditions. *Biochemistry* **1999**, *38*, 13560–73.
- (37) Frangolho, A.; Correia, B. E.; Vaz, D. C.; Almeida, Z. L.; Brito, R. M. M. Oligomerization profile of human transthyretin variants with distinct amyloidogenicity. *Molecules* **2020**, *25*, 5698.
- (38) Gustavsson, A.; Jahr, H.; Tobiassen, R.; Jacobson, D. R.; Sletten, K.; Westermark, P. Amyloid fibril composition and transthyretin gene structure in senile systemic amyloidosis. *Lab. Invest.* **1995**, *73*, 703–708.
- (39) Ihse, E.; Rapezzi, C.; Merlini, G.; Benson, M. D.; Ando, Y.; Suhr, O. B.; Ikeda, S.; Lavatelli, F.; Obici, L.; Quarta, C. C.; Leone, O.; Jono, H.; Ueda, M.; Lorenzini, M.; Liepnieks, J.; Ohshima, T.; Tasaki, M.; Yamashita, T.; Westermark, P. Amyloid fibrils containing fragmented ATTR may be the standard fibril composition in ATTR amyloidosis. *Amyloid.* **2013**, *20*, 142–150.
- (40) Marcoux, J.; Mangione, P. P.; Porcari, R.; Degiacomi, M. T.; Verona, G.; Taylor, G. W.; Giorgetti, S.; Raimondi, S.; Sanglier-Cianferani, S.; Benesch, J. L.; Ceconi, C.; Naqvi, M. M.; Gillmore, J. D.; Hawkins, P. N.; Stoppini, M.; Robinson, C. V.; Pepys, M. B.; Bellotti, V. A novel mechano-enzymatic cleavage mechanism underlies transthyretin amyloidogenesis. *EMBO Mol. Med.* **2015**, *7*, 1337–1349.
- (41) Klimtchuk, E. S.; Prokaeva, T.; Frame, N. M.; Abdullahi, H. A.; Spencer, B.; Dasari, S.; Cui, H.; Berk, J. L.; Kurtin, P. J.; Connors, L. H.; Gursky, O. Unusual duplication mutation in a surface loop of human transthyretin leads to an aggressive drug-resistant amyloid disease. *Proc. Natl. Acad. Sci. U. S. A.* **2018**, *115*, E6428–E6436.
- (42) Dasari, A. K. R.; Arreola, J.; Michael, B.; Griffin, R. G.; Kelly, J. W.; Lim, K. H. Disruption of the CD loop by enzymatic cleavage promotes the formation of toxic transthyretin oligomers through a common transthyretin misfolding pathway. *Biochemistry* **2020**, *59*, 2319–2327.
- (43) Colon, W.; Kelly, J. W. Partial denaturation of transthyretin is sufficient for amyloid fibril formation invitro. *Biochemistry* **1992**, *31*, 8654–8660.
- (44) Takegoshi, K.; Nakamura, S.; Terao, T. 13C–1H dipolar-driven 13C–13C recoupling without 13C rf irradiation in nuclear magnetic resonance of rotating solids. *J. Chem. Phys.* **2003**, *118*, 2325–2341.
- (45) Lee, W.; Tonelli, M.; Markley, J. L. NMR-FAM-SPARKY: Enhanced software for biomolecular NMR spectroscopy. *Bioinformatics* **2015**, *31*, 1325–1327.
- (46) Lai, Z. H.; Colon, W.; Kelly, J. W. The acid-mediated denaturation pathway of transthyretin yields a conformational intermediate that can self-assemble into amyloid. *Biochemistry* **1996**, *35*, 6470–6482.
- (47) Hammarstrom, P.; Jiang, X.; Hurshman, A. R.; Powers, E. T.; Kelly, J. W. Sequence-dependent denaturation energetics: A major determinant in amyloid disease diversity. *Proc. Natl. Acad. Sci. U. S. A.* **2002**, *99* (Suppl. 4), 16427–16432.
- (48) Dasari, A. K. R.; Hughes, R. M.; Wi, S.; Hung, I.; Gan, Z.; Kelly, J. W.; Lim, K. H. Transthyretin aggregation pathway toward the formation of distinct cytotoxic oligomers. *Sci. Rep.* **2019**, *9*, 33.
- (49) Mannini, B.; Mulvihill, E.; Sgromo, C.; Cascella, R.; Khodarahmi, R.; Ramazzotti, M.; Dobson, C. M.; Cecchi, C.; Chiti, F. Toxicity of protein oligomers is rationalized by a function combining size and surface hydrophobicity. *ACS Chem. Biol.* **2014**, *9*, 2309–2317.
- (50) Wang, Y.; Jardetzky, O. Probability-based protein secondary structure identification using combined NMR chemical-shift data. *Protein Sci.* **2002**, *11*, 852–861.
- (51) Cavalli, A.; Salvatella, X.; Dobson, C. M.; Vendruscolo, M. Protein structure determination from NMR chemical shifts. *Proc. Natl. Acad. Sci. U. S. A.* **2007**, *104*, 9615–9620.
- (52) Dasari, A. K. R.; Hung, I.; Michael, B.; Gan, Z.; Kelly, J. W.; Connors, L. H.; Griffin, R. G.; Lim, K. H. Structural characterization of cardiac ex vivo transthyretin amyloid: Insight into the transthyretin misfolding pathway in vivo. *Biochemistry* **2020**, *59*, 1800–1803.
- (53) Ferguson, J. A.; Sun, X.; Dyson, H. J.; Wright, P. E. Thermodynamic stability and aggregation kinetics of EF helix and EF loop variants of transthyretin. *Biochemistry* **2021**, *60*, 756–764.
- (54) Cremades, N.; Chen, S. W.; Dobson, C. M. Structural characteristics of alpha-synuclein oligomers. *Int. Rev. Cell. Mol. Biol.* **2017**, *329*, 79–143.
- (55) Kulenkampff, K.; Wolf Perez, A.; Sormanni, P.; Habchi, J.; Vendruscolo, M. Quantifying misfolded protein oligomers as drug targets and biomarkers in alzheimer and parkinson diseases. *Nature Reviews Chemistry* **2021**, *5*, 277–294.
- (56) Bemporad, F.; Chiti, F. Protein misfolded oligomers: Experimental approaches, mechanism of formation, and structure-toxicity relationships. *Chem. Biol.* **2012**, *19*, 315–327.
- (57) Bergstrom, J.; Gustavsson, A.; Hellman, U.; Sletten, K.; Murphy, C. L.; Weiss, D. T.; Solomon, A.; Olofsson, B. O.; Westermark, P. Amyloid deposits in transthyretin-derived amyloidosis: Cleaved transthyretin is associated with distinct amyloid morphology. *J. Pathol.* **2005**, *206*, 224–232.
- (58) Raimondi, S.; Mangione, P. P.; Verona, G.; Canetti, D.; Nocerino, P.; Marchese, L.; Piccarducci, R.; Mondani, V.; Faravelli, G.; Taylor, G. W.; Gillmore, J. D.; Corazza, A.; Pepys, M. B.; Giorgetti, S.; Bellotti, V. Comparative study of the stabilities of synthetic in vitro and natural ex vivo transthyretin amyloid fibrils. *J. Biol. Chem.* **2020**, *295*, 11379–11387.
- (59) Kingsbury, J. S.; Theberge, R.; Karbassi, J. A.; Lim, A.; Costello, C. E.; Connors, L. H. Detailed structural analysis of amyloidogenic wild-type transthyretin using a novel purification strategy and mass spectrometry. *Anal. Chem.* **2007**, *79*, 1990–1998.
- (60) Abedini, A.; Raleigh, D. P. A role for helical intermediates in amyloid formation by natively unfolded polypeptides? *Phys. Biol.* **2009**, *6*, 015005.
- (61) Anderson, V. L.; Ramlall, T. F.; Rospigliosi, C. C.; Webb, W. W.; Eliezzer, D. Identification of a helical intermediate in trifluoroethanol-induced alpha-synuclein aggregation. *Proc. Natl. Acad. Sci. U. S. A.* **2010**, *107*, 18850–18855.
- (62) Vivoli Vega, M.; Cascella, R.; Chen, S. W.; Fusco, G.; De Simone, A.; Dobson, C. M.; Cecchi, C.; Chiti, F. The toxicity of misfolded protein oligomers is independent of their secondary structure. *ACS Chem. Biol.* **2019**, *14*, 1593–1600.
- (63) Lim, K. H.; Dasari, A. K.; Hung, I.; Gan, Z.; Kelly, J. W.; Wright, P. E.; Wemmer, D. E. Solid-state NMR studies reveal native-like beta-sheet structures in transthyretin amyloid. *Biochemistry* **2016**, *55*, 5272–5278.
- (64) Lim, K. H.; Dasari, A. K. R.; Ma, R.; Hung, I.; Gan, Z.; Kelly, J. W.; Fitzgerald, M. C. Pathogenic mutations induce partial structural changes in the native beta-sheet structure of transthyretin and accelerate aggregation. *Biochemistry* **2017**, *56*, 4808–4818.
- (65) Schmidt, M.; Wiese, S.; Adak, V.; Engler, J.; Agarwal, S.; Fritz, G.; Westermark, P.; Zacharias, M.; Fandrich, M. Cryo-EM structure of a transthyretin-derived amyloid fibril from a patient with hereditary ATTR amyloidosis. *Nat. Commun.* **2019**, *10*, 5008.
- (66) Iakovleva, I.; Hall, M.; Oelker, M.; Sandblad, L.; Anan, I.; Sauer-Eriksson, A. Structural basis for transthyretin amyloid formation in vitreous body of the eye. *Nat. Commun.* **2021**, *12*, 7141.